

The high-resolution LIF spectrum of the SiCCl free radical: Probing the silicon-carbon triple bond

Gretchen Rothschofp, Tony C. Smith, Dennis J. Clouthier*

Ideal Vacuum Products, LLC, 5910 Midway Park Blvd. NE, Albuquerque, NM 87109, United States

ARTICLE INFO

Article history:

Received 25 February 2019

In revised form 4 April 2019

Accepted 9 April 2019

Available online 10 April 2019

Keywords:

Free radical

Fluorescence

Molecular structure

Renner-Teller effect

ABSTRACT

A rotationally resolved spectrum of a band of the $\tilde{A}^2\Sigma^+ - \tilde{X}^2\Pi$ electronic transition of the SiCCl free radical has been obtained for the first time. The radical was produced in an electric discharge jet using 1,1-dichlorosilacyclobutane vapor in high pressure argon as the precursor. The laser-induced fluorescence spectrum of the band system in the 610–550 nm region was recorded and the $^2\Pi_{3/2}$ spin component of the 0–0 band was studied at high resolution. Rotational analysis gave the B values for the combining states and by fixing the CCl bond lengths at *ab initio* values we obtained r'' (Si–C) = 1.692(1) Å and r' (Si–C) = 1.594(1) Å. The bond lengths correspond to a silicon-carbon double bond in the ground state and an unusual Si–C triple bond in the excited state. Single vibronic level emission spectra yielded the ground state bending and stretching energy levels up to energies near 5000 cm^{-1} . These were satisfactorily fitted to a Renner-Teller model that included spin-orbit and vibrational anharmonicity effects.

© 2019 Elsevier Inc. All rights reserved.

1. Introduction

In 2000 the spectra of the jet-cooled SiCH and GeCH free radicals were first identified in the Clouthier laboratory at the University of Kentucky [1]. These radicals turned out to be very interesting from several points of view. One of us (DJC) and Chris Kingston recorded high-resolution rotationally resolved LIF spectra of these species in Anthony Merer's laboratory using his pulse amplified ring dye laser system. By detailed rotational analysis, we showed that both radicals have an Si–C (or Ge–C) double bond in the ground state but this bond contracts by almost 0.1 Å on electronic excitation, forming a triple bond in the excited state [2,3].

Both radicals have a $^2\Pi$ ground state with significant spin-orbit, Renner-Teller (RT) and Fermi resonance complications [4,5]. In GeCH, the spin-orbit coupling constant is large (-388.3 cm^{-1}) and this leads to unusual complexity in the RT effect [5]. The lower $\mu^2\Sigma_{1/2}$ component of the (0,1,0) level is very close to the upper $^2\Pi_{1/2}$ spin-orbit component of (0,0,0) and since they have the same value of $P = \Lambda + l$, they can interact, repelling each other through a process called Sears resonance. We were able to fit all the observed ground state levels by expanding the Renner-Teller matrices to include such resonances.

Subsequently, we collaborated with Tim Steimle at the University of Arizona to measure the dipole moments of SiCH and GeCH [6,7]. Although SiCH has the potential to be an important interstel-

lar molecule, our measured ground state dipole moment of 0.066(2) D presents quite a challenge for microwave and radioastronomy studies. GeCH has measured dipole moments of $\mu(\tilde{X}^2\Pi) = 0.122(2)$ D and $\mu(\tilde{A}^2\Sigma^+) = 1.29(2)$ D and the observed proton magnetic hyperfine splittings gave an upper state Fermi contact parameter of $b_F = 163(2)$ MHz.

Curious about other monosubstituted silicon carbide radicals, in 2002 Evans and Clouthier used *ab initio* theory to predict the ground and excited state properties of the unknown silicon halomethylidyne (SiCX; X = F, Cl, Br) free radicals [8]. The ground state theoretical spin-orbit coupling constants, Renner parameters, and vibrational frequencies were used to generate energy level diagrams for the $\tilde{X}^2\Pi$ states as a guide to future experimental emission studies. In addition, the excited state excitation energies, molecular structures and vibrational frequencies were used to simulate expected band contours for the 0–0 bands of the radicals under typical jet-cooled conditions. Subsequently, Smith, Evans and Clouthier [9] used these theoretical predictions to help find a weak, poorly resolved spectrum of the SiCCl free radical and showed that the *ab initio* results agreed well with experiment.

The search for the spectrum of SiCF turned out to be more arduous than expected. Our calculations suggested that it would be a good target for study, with a significant Renner-Teller effect in the ground state, a silicon-carbon triple bond in the excited state, no isotope complications, and resolvable rotational structure at high resolution. Over some 15 years, the Clouthier and Smith groups made several attempts to record the spectrum of SiCF,

* Corresponding author.

E-mail address: djc@ideavac.com (D.J. Clouthier).

which culminated in the discovery of weak LIF signals in Tony Smith's laboratory at Ideal Vacuum Products. The major difficulty was in finding a suitable precursor [$\text{CF}_3\text{Si}(\text{CH}_3)_3$], but we were ultimately successful in obtaining the $\tilde{A}^2\Sigma^+ - \tilde{X}^2\Pi$ LIF spectrum, rotationally resolving the 0–0 band, deriving approximate ground and excited state molecular structures, and obtained sufficiently resolved emission spectra to study the Renner-Teller effect in some detail [10].

In 2014 & 2015, Céline Léonard and coworkers published two *ab initio* papers [11,12] exploring the rovibronic levels of the ground state of SiCCl and simulating the electronic absorption and emission spectra. These very thorough studies motivated us to attempt to obtain much better spectra of SiCCl than in our previous work. Discovery of a better precursor and substantial advances in technology in the Smith laboratory allowed us to obtain more extensive LIF spectra, record high resolution rotationally resolved spectra of the 0–0 band and greatly enhance our library of emission spectra. The analyses of all these spectra are the subject of the present paper.

2. Experiment

The SiCCl reactive intermediate was generated by seeding the vapor of a suitable precursor into high pressure argon and subjecting pulses of this gas mixture to an electric discharge. As described in detail elsewhere, [13,14] a pulsed molecular beam valve (General Valve, series 9) injected the precursor mixture into a flow channel where an electric discharge between two stainless steel ring electrodes fragmented the precursor, producing the species of interest and a variety of other products. The reactive intermediates were rotationally and vibrationally cooled by free jet expansion into vacuum at the exit of the pulsed discharge apparatus. A 1.0 cm long reheat tube [15] added to the end of the discharge apparatus increased production of the SiCCl radical and suppressed the background glow from excited argon atoms.

Low resolution (3–5 cm^{-1}) survey LIF spectra were recorded using a tunable optical parametric oscillator (OPO) pumped with the 355 nm output of a tripled neodymium: yttrium aluminum garnet (Nd:YAG) laser. In some instances, medium resolution (0.1 cm^{-1}) LIF spectra were obtained with a YAG pumped dye laser (Lumonics HD-500) excitation source. The fluorescence was collected by a lens, focused through appropriate longwave pass filters, and onto the photocathode of a photomultiplier tube (RCA C31034A). The spectra were calibrated with optogalvanic lines from various argon- and neon-filled hollow cathode lamps. The laser-induced fluorescence and calibration spectra were digitized and recorded simultaneously on a homebuilt computerized data acquisition system.

Higher resolution ($\sim 0.013 \text{ cm}^{-1}$ FWHM) LIF spectra were obtained using a pulsed amplified ring dye laser (Coherent 699-21) as the excitation source using DCM Special dye dissolved in ethylene glycol. The amplifier was a Nd:YAG (532 nm) pumped 4-cell system of our own design which was operated with DCM dye in methanol. Absolute wavelength calibration of the CW ring laser, to an estimated accuracy of $\sim 0.001 \text{ cm}^{-1}$, was performed by simultaneously recording the sub-Doppler absorption spectrum of a heated I_2 cell [16]. The IodineSpec5 program was used to calculate the hyperfine transition frequencies [17]. Frequency calibration between the iodine lines was obtained by interpolation between transmission fringes through a pressure-stabilized confocal etalon (free spectral range FSR = 1.5 GHz) whose cavity length was actively locked to a frequency stabilized He–Ne laser.

For emission spectroscopy, LIF band maxima in the SiCCl spectra were excited by the dye laser and the resulting fluorescence was imaged with $f/4$ optics onto the entrance slit of a 0.5 m scan-

ning monochromator (Spex 500 M). The pulsed fluorescence signals were detected with a gated CCD camera (Andor iStar 320 T) and recorded digitally. The emission spectra were calibrated to an estimated accuracy of $\pm 1 \text{ cm}^{-1}$ using emission lines from an argon filled hollow cathode lamp. A 1200 line/mm grating blazed at 750 nm was employed in this work, which gave a bandpass of 29.9 nm with 18 mm effective active area on the CCD.

As in our original work [9], the vapor of trichloro(dichloromethyl)silane ($\text{HCl}_2\text{CSiCl}_3$, Sigma-Aldrich, 96%) diluted with high pressure argon, was initially used as the precursor mixture. This gave very weak SiCCl spectra contaminated by much stronger bands of SiCH, HCCl etc. Fortunately, we discovered that the room temperature vapor of 1,1-dichlorosilacyclobutane ($\text{Cl}_2\text{SiC}_3\text{H}_6$, Sigma-Aldrich, 97%) diluted with argon, was a much better precursor, yielding stronger SiCCl spectra with fewer spectral interferences. The compound was stored in a Pyrex U-tube, pressurized with 40–60 psi of argon, and delivered to the pulsed valve through Teflon tubing. Five mL of the liquid sufficed for all of the experiments reported herein.

3. Results and analysis

3.1. Low resolution LIF spectra

In our previous study [9], we identified six vibronic bands of the $\tilde{A}^2\Sigma^+ - \tilde{X}^2\Pi$ band system of SiC^{35}Cl , each consisting of a prominent transition from the $^2\Pi_{3/2}$ spin component of the ground state and a weaker $^2\Pi_{1/2}$ spin component 158.5 cm^{-1} to lower energy. Four of the bands had measurable Si^{37}Cl isotopic satellites a few wavenumbers to the red. Fig. 1 shows the LIF spectrum obtained in the present study with the new 1,1-dichlorosilacyclobutane precursor and our OPO excitation source. The $^2\Pi_{1/2}$ spin components are very weak in this spectrum due to very efficient cooling in our jet source and will not be discussed further. The 0–0 band was identified as a medium intensity feature just to the red of the intense $^2\Sigma^+ - ^2\Pi_{3/2}$ spin component of the SiCH 3_0^3 band [2]. The inset in Fig. 1 shows the SiCCl 0_0^0 band recorded at 0.1 cm^{-1} resolution, indicating the lack of resolved rotational structure due to the small B value and the intensity relative to nearby weak $^{29}\text{SiCH}$ (4.7%) and $^{30}\text{SiCH}$ (3.1%) 3_0^3 bands.

The LIF spectrum is dominated by a strong progression in ν_1 (Si–C stretch), consistent with the predicted substantial decrease in the Si–C bond length on excitation, which merges with a variety of impurity bands at 1_0^3 . The measured vibrational frequency of 1400.1 cm^{-1} is comparable to the best theoretical estimate of the ν_1 fundamental = 1387.5 cm^{-1} [12] and there is no measurable chlorine isotope effect for these bands. The second prominent feature in the spectrum is a band with a modest 7.1 cm^{-1} isotope shift which we assign as 3_0^1 , giving ν_3 (Si–Cl stretch) = 550.5 cm^{-1} , compared to the *ab initio* fundamental = 541.8 cm^{-1} [12]. Finally, a very weak band without a measurable isotope effect was observed at 15 550 cm^{-1} and assigned as 2_0^1 , giving $\nu_2 = 307.2 \text{ cm}^{-1}$, similar to the *ab initio* fundamental frequency 300.3 cm^{-1} [12]. This band is formally forbidden, but gains intensity through vibronic coupling. The occurrence of such vibronically induced bands following the selection rule $\Delta v_2 = \pm 1$ is not unexpected, as they are also prominent in the spectra of SiCH [2] and SiCF [10].

Once the three fundamental frequencies were established, the rest of the bands in the spectrum were assigned using the slightly anharmonic intervals and chlorine isotope effects. Since some of the weak features may be due to impurity species, emission spectra (*vide infra*) were recorded for all the bands in the 15 000–19 500 cm^{-1} region and the SiCCl bands positively identified by their characteristic ground state frequency intervals. At the beginning of

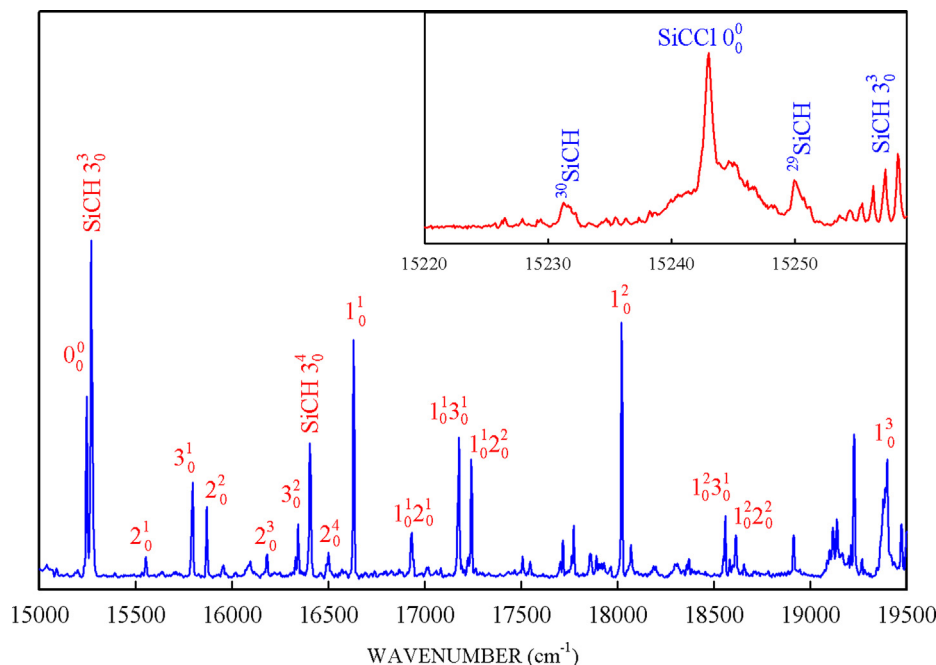


Fig. 1. A low resolution LIF spectrum of the products of an electrical discharge through 1,1-dichlorosilacyclobutane vapor diluted in argon. Most of the bands can be attributed to the SiCHCl free radical ($^2\Pi_{3/2}$ spin-orbit component) although there are impurity bands of SiCH. The blue end of the spectrum is dominated by bands of molecules other than SiCHCl. The inset shows a medium resolution scan of the $^2\Pi_{3/2}$ spin-orbit component of the 0–0 band of SiCHCl and the weak Q-branches of the 3_0^3 ($^2\Sigma^+ - ^2\Pi_{3/2}$) bands of $^{30}\text{SiCH}$ and $^{29}\text{SiCH}$.

the LIF spectrum there is a fairly regular progression of weak bands with a $\sim 310\text{ cm}^{-1}$ interval which we assign as $2_0^1 - 2_0^4$. The 2_0^2 band is more intense than expected and the overtone interval (316.4 cm^{-1}) is larger than the fundamental (307.2 cm^{-1}) suggesting that 2^2 is in Fermi resonance with the 3^1 level slightly below it, in accord with the *ab initio* findings [12]. Combinations of ν_3 and $2\nu_2$ with ν_1 dominate the remainder of the spectrum, with higher bands involving the C–Cl stretch (ν_3) exhibiting ^{37}Cl isotope satellites. The assignments of the observed LIF bands are summarized in Table 1. The band at 17782.2 cm^{-1} is anomalous as there is no near-harmonic combination of frequencies that is very close to this value. However, the chlorine isotope shift of 11.1 cm^{-1} is consistent with an upper state with one quantum of ν_3 (isotope shift = 7.1 cm^{-1}) and two or more quanta of ν_2 ($2\nu_2$ isotope shift

measured previously [9] as 2.2 cm^{-1}). The closest energetically and isotopically feasible assignment is $1_0^1 2_0^2 3_0^1$, which is expected to be about 21 cm^{-1} ($1_0^1 2_0^2 + 550\text{ cm}^{-1}$) higher than observed. The level must be perturbed in some fashion, but the details are ambiguous.

3.2. High-resolution rotationally resolved spectra

Although the observed SiCHCl 0–0 LIF band is quite weak, we were able to obtain a high-resolution spectrum of the $^2\Pi_{3/2}$ component. This involved concatenating a large number of individual 20 GHz ring laser scans, each individually calibrated, to obtain the spectrum shown in Fig. 2. Although some of the central Q-branch features are not well-resolved, the branches on either side show clearly delineated rotational lines. The inset shows a small portion of the P_{11} branch illustrating the resolved Cl isotope splittings. Our previous estimate [9] of the chlorine isotope effect was 0.35 cm^{-1} , comparable to the observed 0.24 cm^{-1} separation of the Q-branch maxima in the spectrum. Although they are obvious in the spectra of SiCH and SiCF, no J-dependent upper state spin-rotation splittings, evident as the difference of the $Q_{21}(J'')$ and $R_{11}(J'')$ lines, were found in the spectrum of SiCHCl.

We have fitted the rotational structure of our spectrum using the very convenient graphical PGopher program [18,19]. Since only one spin component was observed, we fixed the lower state spin-orbit coupling constant A at the value of -158.5 cm^{-1} obtained from the low resolution data (Table 1, ref. [9]). We began by using the predicted rotational constants from our previous *ab initio* work [8] to simulate the spectrum of SiC^{35}Cl , adjusting the band origin to match the position of the Q-branch maximum. The spectra matched quite well, which allowed us to begin the process of assigning lines and fitting the constants. We started out by only fitting the two B values and the band origin. It was soon evident that the ground state A doubling was negligible at our resolution and that the centrifugal distortion constants (D) were not determinable in either state. Since there was no evidence of spin-rotation

Table 1
Assignments and intensity maxima of the observed bands (cm^{-1}) in the LIF spectrum of SiCHCl.

Assign.	$\text{SiC}^{35}\text{Cl } ^2\Pi_{3/2}$	$\text{SiC}^{37}\text{Cl } ^2\Pi_{3/2}$	Comment
0_0^0	15242.80	15242.57 [0.23] ^a	$A_{50} = -158.5$
2_0^1	15550.0		$\nu_2 = 307.2$
3_0^3	15793.3	15786.2 [7.1]	$\nu_3 = 550.5$
2_0^2	15866.4		$2_0^1 + 316.4$
$2_0^3 3_0^1$	16091.4		$2_0^1 + 541.4$
2_0^3	16178.3		$2_0^2 + 311.9$
3_0^3	16337.8	16325.5 [12.3]	$3_0^1 + 544.5$
2_0^4	16496.5		$2_0^2 + 318.2$
1_0^1	16642.9		$\nu_1 = 1400.1$
$1_0^2 2_0^1$	16944.3		$2_0^1 + 1394.3$
$1_0^3 3_0^1$	17188.3	17180.4 [7.9]	$3_0^1 + 1395.0$
$1_0^2 2_0^2$	17253.1		$2_0^2 + 1386.7$
$1_0^1 2_0^3$	17558.7		$2_0^3 + 1380.4$
$1_0^3 3_0^2$	17725.9	17712.5 [13.4]	$3_0^2 + 1388.1$
$1_0^1 2_0^2 3_0^1?$	17782.2	17771.1 [11.1]	Perturbed?
1_0^2	18030.3		$1_0^1 + 1387.4$
$1_0^2 3_0^1$	18565.5	18556.8 [8.7]	$1_0^1 + 535.2$
$1_0^1 2_0^3$	18620.1		$1_0^1 2_0^3 + 1367$
1_0^3	19401.5	–	$1_0^2 + 1371.2$

^a $^{35}\text{Cl} - ^{37}\text{Cl}$ isotope shift.

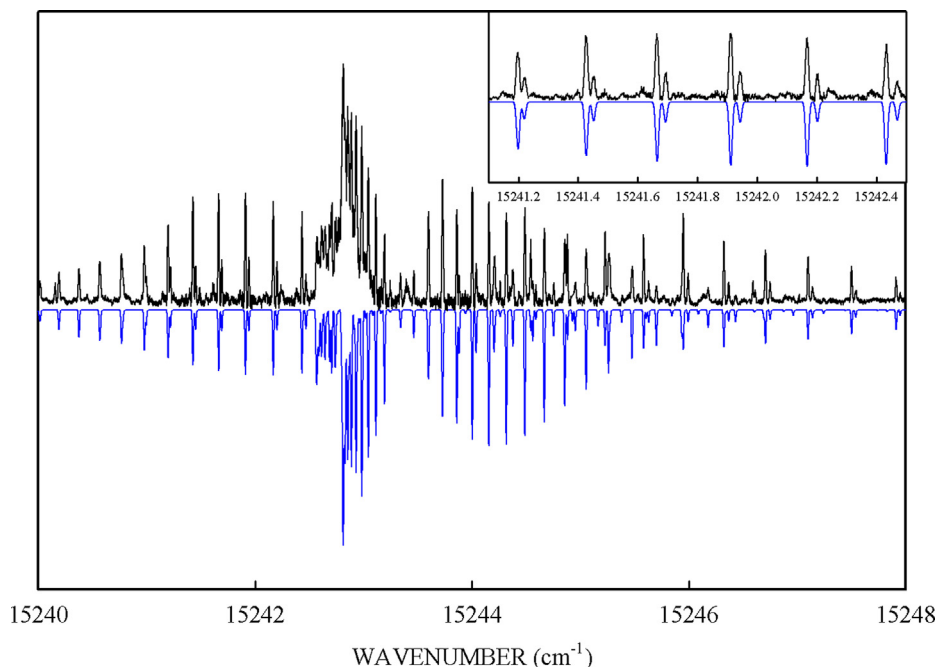


Fig. 2. A high-resolution LIF spectrum of the $^2\Pi_{3/2}$ spin-orbit component of the 0–0 band of SiCl (top) and our simulation of the spectrum with a linewidth of 0.012 cm^{-1} and a rotational temperature of 10 K (bottom). The inset shows a small segment of the P_{11} branches of SiC ^{35}Cl and SiC ^{37}Cl . The experimental spectrum was obtained by concatenating several short segments with varying laser power and experimental conditions, accounting for the irregularity in the baseline. Some weaker features in the spectra not reproduced in the simulation are due to impurity fluorescence.

splittings, only four branches were assignable (R_{11} & Q_{21} overlap as do Q_{11} & P_{21}). Since the spectrum is complicated by the existence of some overlapping ^{37}Cl lines, care had to be taken to ensure that only well-resolved single SiC ^{35}Cl lines were included in the least squares fitting. In the final analysis we varied 3 constants (with A fixed) to fit 54 transitions to an overall standard deviation of 0.00058 cm^{-1} , with the results summarized in Table 3.

The SiC ^{37}Cl spectrum was simulated by the simple expedient of changing the band origin until the Q -branch maximum matched that of experiment. The other branches were then sufficiently close to experiment to begin the assignments. Overlap with the stronger SiC ^{35}Cl transitions was a complicating factor in some regions of the spectrum, but in others (see inset, Fig. 2) the isotopologues were clearly distinguishable. Care was again taken to ensure that only single lines were used in the least squares fitting. Ultimately, we again varied 3 constants to fit 36 transitions with an overall stan-

dard deviation of 0.00053 cm^{-1} . The constants are summarized in Table 3 and the assigned lines of both radicals are given in Table 2. Simulations of the spectra using the fitted constants, a linewidth of 0.012 cm^{-1} and an estimated rotational temperature of 10 K are shown in Fig. 2, illustrating good agreement with the line positions and reasonable reproduction of the relative intensities. No perturbations were detected in any of the branches of the spectrum.

3.3. Emission spectra

In order to study the spin-orbit and RT effects in the ground state, we recorded emission spectra after OPO laser excitation of the $^2\Pi_{3/2}$ spin-orbit components of the 0_0^0 , 2_0^1 , 3_0^1 , 2_0^2 , 2_0^3 , 3_0^2 , 2_0^4 , 1_0^1 , 1_0^2 , 1_0^3 , 1_0^1 , 1_0^2 , 1_0^3 LIF bands. Due to the broad linewidth of the OPO ($3\text{--}6\text{ cm}^{-1}$), the

Table 2
Rotational line frequencies (cm^{-1}) and assignments for the $^2\Sigma^+ - ^2\Pi_{3/2}$ component of the 0–0 band of SiC ^{35}Cl (SiC ^{37}Cl in parentheses).

J''	R_{21}	R_{11} & Q_{21}	Q_{11} & P_{21}	P_{11}
1.5		3.5999*(3.3420* ^a)	3.1940	
2.5	4.5427*(4.2610)	3.7297*(3.4652)	3.1146	2.7074(2.4694)
3.5	4.8812(4.5896)	3.8611(3.5999*)	3.0444	2.4333(2.2025)
4.5	5.2284	4.0044(3.7297*)	2.9851(2.7422*)	2.1677(1.9434)
5.5	5.5844(5.2657*)	4.1569(3.8829)	2.9321(2.6880)	1.9117(1.6936)
6.5	5.9494(5.6301)	4.3181(4.0396)	2.8881*(2.6457)	1.6440(1.4521)
7.5	6.3245(5.9949)	4.4888(4.2079*)	2.8562*(2.6151*)	1.4273(1.2205)
8.5	6.7078(6.3684)	4.6686(4.3778)	2.8297*(2.5877)	1.1979(0.9951)
9.5	7.1001(6.7506)	4.8571(4.5608)	2.8131*	0.9787(0.7821)
10.5	7.5015(7.1413)	5.0551*(4.7552*)	2.8131*	0.7692
11.5	7.9126(7.5403)	5.2655*(4.9542)	2.8131*	0.5689
12.5	8.3324(7.9497)	5.4792*(5.1683*)		0.3759
13.5	8.7619(8.3663)	5.7017		0.1921
14.5	9.2002(8.7930)	5.9352		0.0162*
15.5	9.6455*	6.1788		
16.5		6.4317		

^aThe actual transition frequencies can be obtained by adding 15240 cm^{-1} to each entry in the table. An asterisk denotes a blended or otherwise poor line not used in the least squares fitting.

Table 3
The molecular constants (in cm^{-1}) of SiCCl.

Parameter	$^2\Pi$		$^2\Sigma^+$	
	SiC ^{35}Cl	SiC ^{37}Cl	SiC ^{35}Cl	SiC ^{37}Cl
T_0	–	–	15164.03276(36)	15163.78173(45)
B	0.097520 ₆ (13) ^a	0.095147 ₄ (22)	0.102017 ₃ (12)	0.099489 ₁ (17)
A	–158.5 ^b	–158.5 ^b	–	–

^a The numbers in parentheses are 3σ error limits and are right-justified to the last digit on the line; sufficient additional digits are quoted to reproduce the original data to full accuracy.

^b Value taken from Table 1 and fixed in the least squares fitting.

excitation was over most of the rotational structure of each band. Since the detector was a gated CCD, we were able to eliminate all scattered laser light, even at the laser excitation wavenumber, by delaying the exposure until a few ns. after the laser pulse. Although we were able to calibrate the spectra using argon atomic emission lines to better than 0.5 cm^{-1} in each case, the SiCCl emission bands were $7\text{--}8 \text{ cm}^{-1}$ wide and could not be measured reproducibly to better than $\pm 1 \text{ cm}^{-1}$ and displacements (a direct measure of ground state energy = laser excitation – emission feature, cm^{-1}) to $\pm 1\text{--}2 \text{ cm}^{-1}$.

In the SiCCl $^2\Pi$ ground state, the vibrations are labeled ν_1^+ = SiC stretch, ν_2^- = bend and ν_3^- = CCl stretch. The vibrational levels are split into components by a combination of RT and spin–orbit interactions and the levels are denoted by $K = \Lambda + l$ with the term symbols Σ ($K = 0$), Π ($K = 1$), Δ ($K = 2$) etc. and a half-integer subscript $P = K + \Sigma$. The labels μ and κ are used to denote lower and upper levels, respectively, that have the same values of K and P . As every level has the same spin multiplicity of 2, we have suppressed the usual superscript value of 2 before every term symbol.

Some examples of the data are shown in Fig. 3. The top trace illustrates the emission spectrum obtained after OPO excitation of the 0_0^0 band. Each transition consists of two features of nearly equal intensity, to the lower $\Pi_{3/2}$ and upper $\Pi_{1/2}$ spin–orbit components of each lower state stretching level. The spectrum exhibits

a short progression in ν_3^- (526.4 cm^{-1} , C–Cl stretch) and a prominent 1_0^0 band with $\nu_1^+ = 1274.4 \text{ cm}^{-1}$ (Si–C stretch). The 3_0^2 band exhibits measurable ^{37}Cl features 12 cm^{-1} to lower energy. The remainder of the spectrum can be assigned as transitions to combination of ν_1^+ and ν_3^- . A few very weak features might plausibly be attributed to transitions to bending levels.

The 2_0^1 band emission spectrum (middle trace in Fig. 3) is very different and contains much more information about the bending levels and the RT effect. As a result of the general selection rules $\Delta l = 0$, $\Delta K = \Delta \Lambda = \pm 1$, it is expected that 2_1^1 will emit predominantly to levels with $\Delta \nu_2 = 0, \pm 2$. As a result the transition back down to $\nu_2'' = 0$ is very weak and the 2_1^1 band is strong, exhibiting barely resolved features down to all four components ($\mu\Sigma$, $\Delta_{5/2}$, $\Delta_{3/2}$ and $\kappa\Sigma$) of the 2_1 state, data which basically defines the RT parameter ϵ . This pattern repeats with combinations of 2_1 and the stretching levels out to $1_1 2_1 3_1$ at a displacement of 2005.6 cm^{-1} .

Finally, the bottom trace shows the emission spectrum obtained by excitation of the 3_0^2 band. This emission spectrum is again quite different and shows strong activity in even quanta of ν_2'' , as well as emission to 3_1 and 1_1 . The bending levels beyond two quanta are complicated by near-degeneracies, as shown in Fig. 4, which illustrates the observed levels and the emission spectra from laser excitation of the 2_0^2 , 2_0^3 and 2_0^4 transitions. We note that the weak 2_0^3 and 2_0^4 bands are overlapped by the $3_0^2 \Pi_{1/2}$ and $1_0^1 \Pi_{1/2}$ spin–orbit

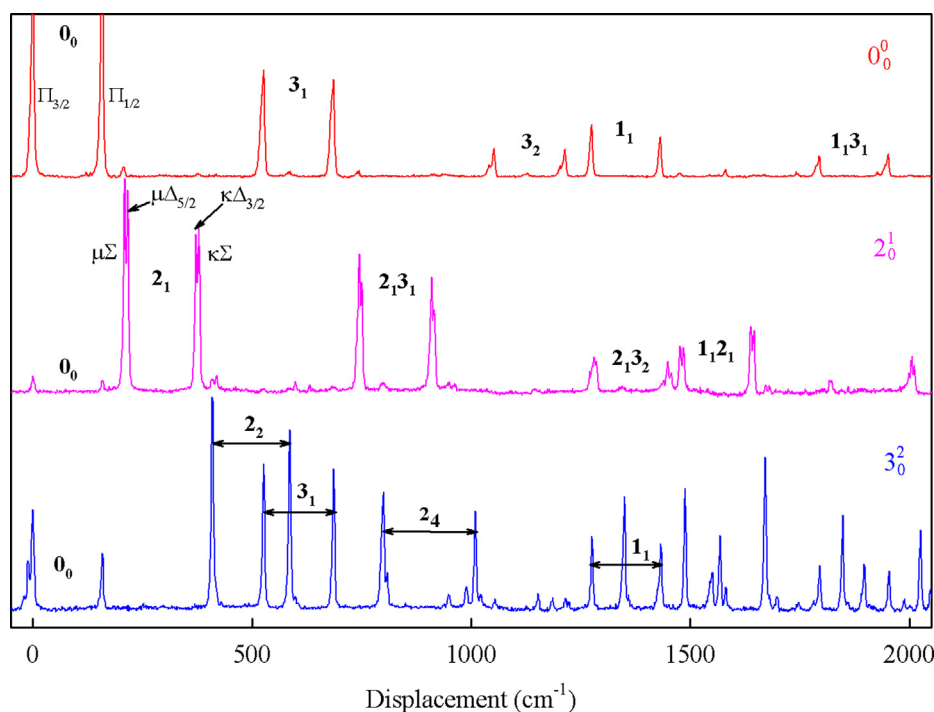


Fig. 3. The emission spectra observed from laser excitation of the $^2\Pi_{3/2}$ spin–orbit components of the 0_0^0 , 2_0^1 , and 3_0^2 bands of SiCCl. The horizontal scale is displacement from the excitation laser wavenumber, giving a direct measure of the relative ground state energy of each transition.

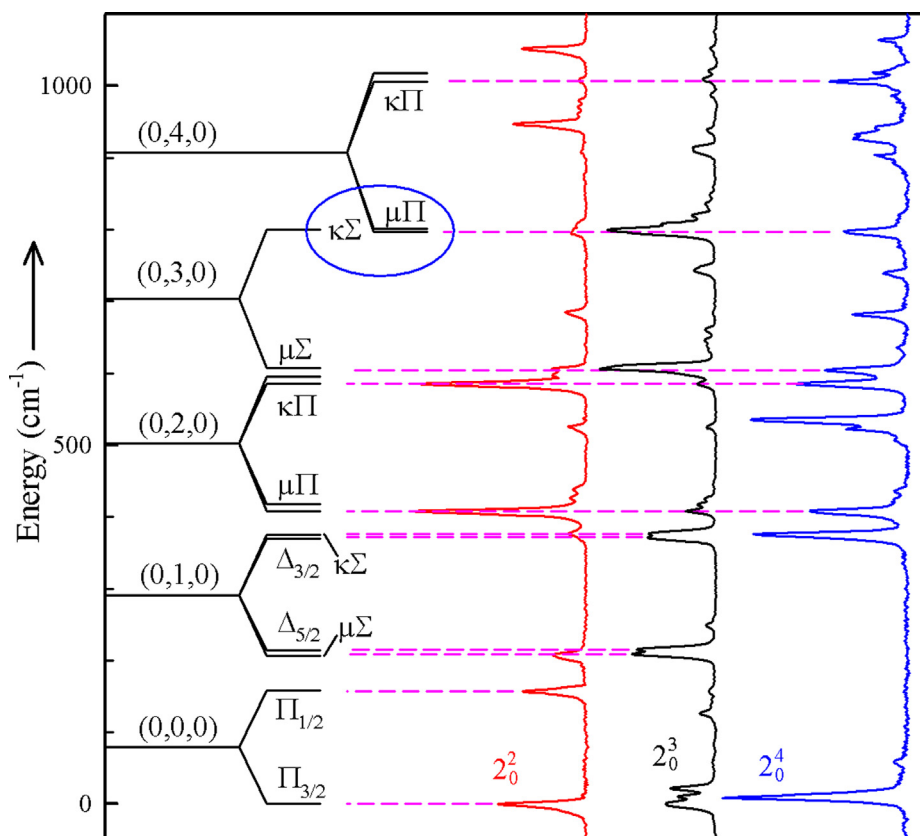


Fig. 4. The experimentally derived ground state bending energy levels of SiC^{35}Cl (LHS) compared to the emission spectra obtained by laser pumping of the 2_0^2 , 2_0^3 and 2_0^4 bands of SiCl (RHS). The vertical scale is displacement from the excitation laser wavenumber, giving a direct measure of the relative ground state energy of each transition. Horizontal dashed lines indicate the correspondence of the energy levels to the observed transitions. The oval identifies the upper levels of (0,3,0) and the lower levels of (0,4,0) which are in close proximity and are predicted to interact [11]. For states above (0,1,0), some of the energy levels have been omitted for clarity.

components, which complicate the emission spectra, fortunately in a predictable fashion. As shown in the Figure, the 2_0^2 band emits strongly to the 0_0 and 2_2 levels and weakly to 2_1 , 2_3 and 2_4 . In sharp contrast and in accord with the vibrational selection rules, the 2_0^0 band emission terminates predominantly on 2_1 and 2_3 , picking out the latter among the nearby 2_2 and 2_4 levels. Finally, the 2_0^4 band emission spectrum terminates on 2_2 and 2_4 , with complications due to the excitation of the overlapping transition to the 1^1 stretching level. Careful analysis of these three spectra allowed us to identify ground state levels up to four quanta of the bend. These also show up in combination bands in the emission spectra from various other excited state levels.

We have fitted our data to a Renner-Teller model including spin-orbit and Fermi resonance complications, using a computer program [20] written especially for this purpose and employed previously to analyze similar emission data for SiCH [4], GeCH [5] and SiCF [10]. Initially, we fitted only the bending levels up to 2_4 varying only the average bending frequency, ω_2 , the bending frequency times the Renner-Teller parameter, $\epsilon\omega_2$, the spin-orbit coupling constant, A , and the primary bending anharmonicity constant, g_4 . These fitted quite well, although assignments in the regions of the overlapping 2_3 and 2_4 levels were quite difficult. Subsequently, we added the levels 3_1 – 3_4 , which defined ω_3 and proved to have negligible anharmonicity. The Si–C stretching levels 1_1 – 1_4 proved more difficult and required both a substantial anharmonic constant, x_{11} , and explicit allowance for the variation of the spin-orbit interaction with excitation of the ν_1' vibration:

$$A_\nu = A - a_1^A \nu_1 \quad (1)$$

The latter can be seen from the variation in the observed spin-orbit splitting of the ν_1' levels, which decreases monotonically from 0_0 to 1_4 as 158.5, 157.1, 156.3, 153.7 and 151.1 cm^{-1} .

Once this basic framework was established, the energy levels involving various combinations of the three ground state vibrations were added to the least squares analysis. In the process, the anharmonic constants x_{12} , x_{13} , and x_{23} were found to be necessary to fit the data. Eventually, 102 ground state energy levels were assigned and 97 were fitted to an overall standard deviation of 2.29 cm^{-1} which is very satisfactory for a Renner-Teller analysis. The fitted levels and their least squares residuals are given in Table 4 and the resulting constants are summarized in Table 5. There was no evidence of significant Fermi resonance interactions in the data.

4. Discussion

4.1. The molecular structure of SiCl

It is abundantly clear from the spectrum that SiCl is a linear molecule. Initially we had hoped that the two slightly different B values from SiC^{35}Cl and SiC^{37}Cl would allow us to accurately determine complete r_0 structures in both states. However, the data were insufficiently precise to do so; the structure determinations had large error bars and unrealistic values, as judged from the comparison with *ab initio* geometric parameters [11,12]. We then resorted to fixing the C–Cl values at their best theoretical bond lengths [11,12] and varying the Si–C bond length to match the rotational

Table 4
Vibrational levels of the $\bar{X}^2\Pi_i$ state of SiC³⁵Cl (in cm⁻¹ relative to the lowest (0 0 0) $^2\Pi_{3/2}$ level).

State (v_1, v_2, v_3)	Energy	Obs. - Calc. ^a	State (v_1, v_2, v_3)	Energy	Obs. - Calc. ^a
(0,0,0) $\kappa\Pi_{1/2}$	158.5	-0.11	(1,2,0) $\kappa\Pi_{1/2}$	1845.7	-3.01
(0,1,0) $\mu\Sigma_{1/2}$	206.6	-2.06	(1,3,0) $\mu\Sigma_{1/2}$	1862.1	-0.02
(0,1,0) $\mu\Delta_{5/2}$	213.7	1.31	(1,3,0) $\mu\Delta_{5/2}$	1866.0	2.13
(0,1,0) $\kappa\Delta_{3/2}$	369.4	0.27	(0,1,3) $\kappa\Delta_{3/2}$	1989.4*	14.49
(0,1,0) $\kappa\Sigma_{1/2}$	375.6	-1.96	(0,1,3) $\kappa\Sigma_{1/2}$	1996.3*	13.49
(0,2,0) $\mu\Pi_{3/2}$	408.0	-2.49	(1,1,1) $\mu\Sigma_{1/2}$	2003.8	-1.05
(0,2,0) $\mu\Pi_{1/2}$	418.0	2.33	(1,1,1) $\mu\Delta_{5/2}$	2009.5	0.89
(0,0,1) $\mu\Pi_{3/2}$	526.4	-1.21	(1,3,0) $\kappa\Delta_{3/2}$	2050.1	2.63
(0,2,0) $\kappa\Pi_{1/2}$	585.3	-2.59	(1,3,0) $\kappa\Sigma_{1/2}$	2059.2	1.36
(0,2,0) $\kappa\Pi_{3/2}$	595.3	1.00	(0,0,4) $\mu\Pi_{3/2}$	2109.9	-0.54
(0,3,0) $\mu\Sigma_{1/2}$	607.1	0.37	(1,1,1) $\kappa\Delta_{3/2}$	2166.6	2.32
(0,3,0) $\mu\Delta_{5/2}$	610.6	2.05	(1,1,1) $\kappa\Sigma_{1/2}$	2173.3	0.59
(0,0,1) $\kappa\Pi_{1/2}$	685.3	-0.99	(1,2,1) $\mu\Pi_{3/2}$	2203.6	-4.01
(0,1,1) $\mu\Sigma_{1/2}$	742.5	-1.21	(0,0,4) $\kappa\Pi_{1/2}$	2279*	9.73
(0,1,1) $\mu\Delta_{5/2}$	747.0	-0.46	(1,0,2) $\mu\Pi_{3/2}$	2313.5	-1.96
(0,4,0) $\mu\Pi_{3/2}$	797.1	3.08	(1,2,1) $\kappa\Pi_{1/2}$	2381.7	-2.36
(0,3,0) $\kappa\Sigma_{1/2}$	800.1	-3.37	(1,0,2) $\kappa\Pi_{1/2}$	2472.2	-0.83
(0,3,0) $\kappa\Delta_{5/2}$	809.8	1.11	(1,1,2) $\mu\Sigma_{1/2}$	2534.3	1.83
(0,1,1) $\kappa\Delta_{3/2}$	906.0	1.58	(2,0,0) $\mu\Pi_{3/2}$	2535.5	-1.07
(0,1,1) $\kappa\Sigma_{1/2}$	912.6	-0.06	(1,1,2) $\mu\Delta_{5/2}$	2539.7	3.44
(0,2,1) $\mu\Pi_{3/2}$	948.2	-4.85	(2,0,0) $\kappa\Pi_{1/2}$	2691.8	-1.01
(0,2,1) $\mu\Pi_{1/2}$	961.9	3.80	(1,1,2) $\kappa\Delta_{3/2}$	2693.5	1.36
(0,4,0) $\kappa\Pi_{1/2}$	1006.5	-0.51	(1,1,2) $\kappa\Sigma_{1/2}$	2705.7	5.32
(0,4,0) $\kappa\Pi_{3/2}$	1018.3	2.43	(2,1,0) $\mu\Sigma_{1/2}$	2733.0	0.81
(0,0,2) $\mu\Pi_{3/2}$	1052.9	-2.32	(2,1,0) $\mu\Delta_{5/2}$	2739.8	3.87
(0,2,1) $\kappa\Pi_{1/2}$	1128.0	-2.62	(1,0,3) $\mu\Pi_{3/2}$	2832.8	-2.85
(0,3,1) $\mu\Sigma_{1/2}$	1153.1	-3.66	(2,1,0) $\kappa\Delta_{3/2}$	2892.0	1.98
(0,3,1) $\mu\Delta_{5/2}$	1156.2	-2.49	(2,1,0) $\kappa\Sigma_{1/2}$	2898.8	-0.09
(0,0,2) $\kappa\Pi_{1/2}$	1213.5	-0.46	(2,2,0) $\mu\Pi_{3/2}$	2918.5	-2.32
(1,0,0) $\mu\Pi_{3/2}$	1274.4	-0.68	(1,0,3) $\kappa\Pi_{1/2}$	2995.2	1.92
(0,1,2) $\mu\Sigma_{1/2}$	1278.1	-0.65	(2,0,1) $\mu\Pi_{3/2}$	3049.6	0.26
(0,1,2) $\mu\Delta_{2.5}$	1282.3	-0.22	(2,2,0) $\kappa\Pi_{1/2}$	3094.1	-1.80
(0,3,1) $\kappa\Delta_{3/2}$	1344.4	0.39	(2,0,1) $\kappa\Pi_{1/2}$	3205.9	0.24
(0,3,1) $\kappa\Sigma_{1/2}$	1349.2	-4.46	(2,1,1) $\mu\Sigma_{1/2}$	3253.0	0.60
(0,3,1) $\kappa\Delta_{5/2}$	1359.3	0.73	(2,1,1) $\mu\Delta_{5/2}$	3259.6	3.43
(1,0,0) $\kappa\Pi_{1/2}$	1431.5	-1.01	(2,1,1) $\kappa\Delta_{3/2}$	3414.2	3.67
(0,1,2) $\kappa\Delta_{3/2}$	1446.6*	6.92	(2,1,1) $\kappa\Sigma_{1/2}$	3421.1	1.94
(0,1,2) $\kappa\Sigma_{1/2}$	1452.6	4.86	(2,2,1) $\mu\Pi_{3/2}$	3444.5	-4.06
(1,1,0) $\mu\Sigma_{1/2}$	1475.0	-2.23	(2,2,1) $\kappa\Pi_{1/2}$	3621.0	-2.88
(1,1,0) $\mu\Delta_{5/2}$	1482.6	1.64	(2,0,2) $\mu\Pi_{3/2}$	3559.9	-2.21
(0,2,2) $\mu\Pi_{3/2}$	1488.1*	-7.49	(2,0,2) $\kappa\Pi_{1/2}$	3717.2	-1.31
(0,4,1) $\kappa\Pi_{1/2}$	1568.0	2.81	(3,0,0) $\mu\Pi_{3/2}$	3784.3	-0.17
(0,0,3) $\mu\Pi_{3/2}$	1579.5	-3.33	(3,0,0) $\kappa\Pi_{1/2}$	3938.0	-1.50
(1,1,0) $\kappa\Delta_{3/2}$	1636.2	-0.19	(3,0,1) $\mu\Pi_{3/2}$	4289.7	-0.12
(1,1,0) $\kappa\Sigma_{1/2}$	1642.3	-2.73	(3,0,1) $\kappa\Pi_{1/2}$	4444.7	-0.25
(0,2,2) $\kappa\Pi_{1/2}$	1670.2	-3.12	(3,0,2) $\mu\Pi_{3/2}$	4794.1	-1.06
(1,2,0) $\mu\Pi_{3/2}$	1670.2	-2.26	(3,0,2) $\kappa\Pi_{1/2}$	4950.4	0.02
(1,2,0) $\mu\Pi_{1/2}$	1680.5	2.75	(4,0,0) $\mu\Pi_{3/2}$	5020.5	1.74
(0,0,3) $\kappa\Pi_{1/2}$	1742.5	0.88	(4,0,0) $\kappa\Pi_{1/2}$	5171.6	-0.99
(0,1,3) $\mu\Sigma_{1/2}$	1818.0	4.21	(4,0,1) $\mu\Pi_{3/2}$	5516.8	0.11
(0,1,3) $\mu\Delta_{5/2}$	1819.9	2.32	(4,0,1) $\kappa\Pi_{1/2}$	5671.3	0.67

^a From our Renner-Teller analysis of the emission spectra. An asterisk denotes a blended or otherwise uncertain level not used in the least squares fitting. The μ and κ labels are those from our computer program and are not consistent with general usage. For example, although (0,0,0) $\kappa\Pi_{1/2}$ is the upper spin-orbit component, the lower spin-orbit component is (0,0,0) $\Pi_{3/2}$ which does not have the same value of P , so the μ , κ notation is not strictly relevant.

constants of both SiC³⁵Cl and SiC³⁷Cl. In this fashion we obtained $r'' = 1.696(1)$ Å and $r' = 1.599(1)$ Å, as summarized in Table 5.

The ground state Si–C bond lengths of SiCH [2], SiCF [10] and SiCl are 1.693(1), 1.693(1) and 1.696(1) Å, respectively. Clearly, halogenation has little effect on the bond length. Silicon-carbon single bonds are much longer, of the order of 1.87–1.91 Å [21]. We determined the length of the silicon-carbon double bond in transient silylidene (H₂C=Si) [22] to be 1.706 Å, very similar to the 1.7039 Å value in highly reactive gas phase H₂Si=CH₂ [23,24], and both only 0.014–0.012 Å longer than in the SiCX free radicals. The SiC radical with a $\pi^3\sigma^1$ ($^3\Pi$) configuration has $r_e = 1.7182(2)$, consistent with a long silicon-carbon double bond [25]. Several stable silicon-carbon doubly bonded molecules have also been reported [21]. These invariably have large bulky substituents to tame their inherent reactivity, with typical bond lengths ranging from 1.702 to 1.764 Å. All the evidence points to a short silicon-carbon double bond in the SiCX species. In the

excited state, this bond contracts by almost 0.1 Å in all cases. To our knowledge, there are no known stable molecules with carbon-silicon triple bonds, but theory predicts a value of 1.604 Å for linear HC≡SiH [26], very close to the excited state values of SiCH = 1.6118(1) Å, SiCF = 1.594(1) Å and SiCl = 1.599(1) Å, which are consistent with a triple bond.

These conclusions can be understood from the molecular orbitals involved. In the ground state of SiCX, the electron configuration is $\dots(\sigma_b)^2(\sigma_{nb})^2(\pi)^3(^2\Pi_i)$, where σ_b is a Si–C bonding orbital, σ_{nb} is a nonbonding lone pair on the silicon atom and the π orbitals are Si–C bonding. The filled σ_b orbital and partially filled π orbitals result in a short double bond in the ground state. The first electronic excited state is formed by promotion of an electron from the nonbonding orbital to the π bonding orbitals, yielding the configuration $\dots(\sigma_b)^2(\sigma_{nb})^1(\pi)^4(^2\Sigma^+)$ which now has a total of six electrons in bonding orbitals, forming a carbon-silicon triple bond.

Table 5
Experimental and *ab initio* spectroscopic parameters (cm^{-1} unless otherwise noted) of SiC^{35}Cl .

Parameter	$\tilde{X}^2\Pi$		$\tilde{A}^2\Sigma^+$	
	Experiment ^a	<i>Ab Initio</i> ^b	Experiment ^c	<i>Ab Initio</i> ^d
T_0	0	0	15164.03	14863.7
ω_1 (Si–C stretch)	1281.34(82)	1293.2	1400.19 ^d	1392.2
ω_2 (bend)	219.08(81)	216.5	307.2	304.6
ω_3 (C–Cl stretch)	527.59(30)	520.7	550.5	563.1
RT parameter, ε	−0.1281(22)	−0.145	–	–
α_4^A	−1.12(45)	–	–	–
g_4	−1.237(80)	–	–	–
x_{11}	−6.80(22)	–	–	–
x_{12}	−6.47(33)	–	–	–
x_{13}	−7.42(26)	–	–	–
x_{23}	7.41(29)	–	–	–
x_{33}	–	–	–	–
Spin-orbit coupling constant, A	−159.48(77)	−162.205	–	–
C–Cl bond length (Å)	–	1.637	–	1.657
SiC bond length (Å)	1.696(1) ^e	1.692	1.599(1) ^e	1.614

^a From our Renner-Teller analysis of the emission spectra. The numbers in parenthesis are 1σ standard errors.

^b *Ab initio*, ref [11].

^c From our analysis of the LIF spectrum, this work.

^d *Ab initio*, ref [12].

^e From our analysis of the high-resolution LIF spectrum, C–Cl bond length fixed at *ab initio* value.

4.2. Rotational and vibrational analysis

No spin-rotation splittings were resolved in our high-resolution spectrum of SiCCl. In the pure precession approximation, the predominant contribution to the excited state spin-rotation parameter γ would come from the interaction with the $^2\Pi_1$ ground state, given by the relation

$$\gamma = 2ABl(l+1)/(E_{\Pi} - E_{\Sigma}) \quad (2)$$

where A is the spin-orbit coupling constant, l is the angular momentum quantum number of the electron that gives rise to the Σ and Π states and B is the rotational constant of the Σ state. The calculated value is $4.3 \times 10^{-3} \text{ cm}^{-1}$ which would lead to resolvable spin-rotation splittings at our resolution. However, previous experience with SiCH [2] and SiCF [10] shows that the pure precession approximation overestimates γ by 1.6 (SiCH) to 2.4 times (SiCF). If we somewhat arbitrarily scale the SiCCl value by a factor of 4 yielding $\gamma \approx 1 \times 10^{-3} \text{ cm}^{-1}$, we find that the spin-rotation splittings would be barely resolvable among the weak features at the high energy end of the spectrum, entirely consistent with experiment.

The SiC^{35}Cl B_0 values obtained in our rotational analysis can be compared to those from the best available *ab initio* calculations [11,12]. The difference is 0.08% for the ground state and 1.2% for the excited state, very good agreement. As shown in Table 5, the calculated excited state vibrational fundamentals are also in excellent agreement with experiment and T_0 is slightly low by only 300 cm^{-1} (2%). Finally, theory reproduces the ground state spin-orbit coupling constant with high fidelity, overestimating by only 1.0 cm^{-1} or 0.6%.

In comparing the *ab initio* calculated energy levels of the ground state of SiC^{35}Cl [11] with our experimental values (Table 4), we find excellent agreement. The general trend is for the theoretical levels to be a few cm^{-1} lower in energy than experiment, a consequence of the slightly lower theoretical values for ω_2 and ω_3 . Although our assignments of the emission spectra purposely did not rely on the theoretical predictions, we find that the two in very good accord. As predicted *a priori* by theory [11], the ground state energy levels in the 750–850 cm^{-1} region caused us considerable difficulty, due to near degeneracies in some of the bending levels, as shown in Fig. 4. The upper levels of 2_3 and the lower levels of 2_4 overlap in this region and are coupled [11], leading to some ambiguity in making assignments. Those in Table 4 are our best

efforts that fit the RT Hamiltonian but they may be slightly in error. We also found that, although the assignments seem solid, the κ (0,1,3) $\Delta_{3/2}$ and Σ levels at 1989.4 and 1996.3 cm^{-1} do not fit our model, with errors of about $+14 \text{ cm}^{-1}$, but agree well with the theoretical values of 1995.7 and 2003.9 cm^{-1} . The cause of this discrepancy is unclear. In a similar fashion, assigned levels at 1446.0, 1488.1 and 2279.0 cm^{-1} (see Table 4) were removed from the final least squares fitting as they had anomalously large residuals. Finally, we note that the theoretical values are reliable even at quite high vibrational energies; the (3,0,0) $^2\Pi_{3/2}$ and $^2\Pi_{1/2}$ levels have expt – theoretical values of -8.5 and -10.3 cm^{-1} , respectively [27].

Two other aspects of our Renner-Teller analysis deserve comment. The first is that the x_{23} anharmonicity constant is large and positive ($=7.4 \text{ cm}^{-1}$). Such a positive anharmonicity between the bending and lowest stretching levels is not uncommon as $x_{23} = 5.6 \text{ cm}^{-1}$ for SiCF [10] and 1.26 for GeCD [5]. The second is the finding that g_K could not be determined from the plethora of experimental data for SiCCl. This is a bit unusual as this constant, which is a measure of the K dependence of the mixing of the vibrational levels of the Π state with those of other Σ and Δ states, is found to have values of SiCH = $10.8(2) \text{ cm}^{-1}$, SiCD = $6.6(2) \text{ cm}^{-1}$ [4] and SiCF = $3.0(8) \text{ cm}^{-1}$ [28]. There is no *a priori* method of calculating a g_K value for SiCCl but Jungen and coworkers have used a simple model in which the $^2\Pi$ state is only coupled to the nearby $^2\Sigma^+$ state and derived

$$g_K = \frac{-\varepsilon_1 \omega^2}{2\Delta E_{\Sigma\Pi}(1 + \varepsilon_1)} \quad (3)$$

where ε_1 is a parameter which depends on the electronic radial factors of the interacting states, their energy difference and the force constant k of the doubly degenerate harmonic oscillator in the RT model. The quantities ΔE and ω in Eq. (3) are the energy difference between the $^2\Sigma^+$ and $^2\Pi$ states and the Π state bending frequencies, respectively. Ignoring the effect of ε_1 , whose magnitude is generally unknown, we might expect that g_K would scale as ω^2 , and this is roughly the case. A plot of g_K vs $\omega^2/2\Delta E$ for the silicon-containing radicals yields a good straight line which extrapolates to $g_K \approx 2.4 \text{ cm}^{-1}$ for SiCCl. Since g_K was barely determined in the case of SiCF, it is perhaps not surprising that it was not statistically determinable for SiCCl.

The ${}^2\Pi_i$ ground state vibrational levels of SiCH, SiCF and SiCCl are now well understood. In SiCH, the spin-orbit coupling constant ($A = -71.9 \text{ cm}^{-1}$) is rather small so the angular momentum coupling (RT effect) shows up as easily resolved splittings between the $\mu\Sigma$ and $\Delta_{5/2}$ (39.6 cm^{-1}) components of 2_1 . Although the RT parameters are similar in all three radicals, the decreasing value of ω_2 and the increasing magnitude of the spin-orbit coupling constant make the same splittings much smaller in SiCF (15 cm^{-1}) and SiCCl (7 cm^{-1}). In all these radicals the RT effects are moderate but as the mass of the halogen increases, the level splittings are dominated by the spin-orbit coupling.

5. Conclusions

Due to improvements in technology and the discovery of a better precursor, our original analysis of the $\tilde{A} \ ^2\Sigma^+ - \tilde{X} \ ^2\Pi$ electronic transition of the SiCCl free radical has been greatly enhanced. More extensive LIF spectra have been obtained and the upper state vibrational levels thoroughly documented. A plethora of well-resolved high quality emission spectra have been recorded, and the ground state vibronic energy levels assigned up to as high as 5000 cm^{-1} . The measured $\tilde{X} \ ^2\Pi$ energy levels were fitted to a Renner-Teller model which allowed the determination of the vibrational frequencies, anharmonicities, Renner-Teller parameter, and spin-orbit coupling constant. In addition, we were able to obtain high-resolution spectra of the ${}^2\Pi_{3/2}$ spin-orbit component of the 0–0 bands of SiC ^{35}Cl and SiC ^{37}Cl . The B values allowed a determination of the linear molecule silicon-carbon bond lengths as $r''(\text{Si}-\text{C}) = 1.696(1) \text{ \AA}$ and $r'(\text{Si}-\text{C}) = 1.599(1) \text{ \AA}$ with $r(\text{C}-\text{Cl})$ fixed at the most recent *ab initio* values [11,12]. Combined with our previous analyses of the spectra of SiCH and SiCF, these data show that the SiCX free radicals have a silicon-carbon double bond in the ground state and an unusual silicon-carbon triple bond in the excited state.

Acknowledgements

DJC is grateful to Dr. Céline Léonard for correspondence and advice concerning their *ab initio* studies of the energy levels and

spectrum of the SiCCl free radical. This research was funded by Ideal Vacuum Products.

References

- [1] T.C. Smith, H. Li, D.J. Clouthier, *J. Am. Chem. Soc.* 121 (1999) 6068.
- [2] T.C. Smith, H. Li, D.J. Clouthier, C.T. Kingston, A.J. Merer, *J. Chem. Phys.* 112 (2000) 3662.
- [3] T.C. Smith, H. Li, D.J. Clouthier, C.T. Kingston, A.J. Merer, *J. Chem. Phys.* 112 (2000) 8417.
- [4] T.C. Smith, H. Li, D.A. Hostutler, D.J. Clouthier, A.J. Merer, *J. Chem. Phys.* 114 (2001) 725.
- [5] S. He, H. Li, T.C. Smith, D.J. Clouthier, A.J. Merer, *J. Chem. Phys.* 119 (2003) 10115.
- [6] T.C. Smith, D.J. Clouthier, T.C. Steimle, *J. Chem. Phys.* 115 (2001) 817.
- [7] T.C. Smith, D.J. Clouthier, T.C. Steimle, *J. Chem. Phys.* 115 (2001) 5047.
- [8] C.J. Evans, D.J. Clouthier, *J. Chem. Phys.* 117 (2002) 6439.
- [9] T.C. Smith, C.J. Evans, D.J. Clouthier, *J. Chem. Phys.* 117 (2002) 6446.
- [10] G. Rothschof, T.C. Smith, D.J. Clouthier, *J. Chem. Phys.* 149 (2018) 024301.
- [11] V. Brites, A.O. Mitrushchenkov, K.A. Peterson, C. Léonard, *J. Chem. Phys.* 141 (2014) 034305.
- [12] A.O. Mitrushchenkov, V. Brites, C. Léonard, *Mol. Phys.* 113 (2015) 1695.
- [13] H. Harjanto, W.W. Harper, D.J. Clouthier, *J. Chem. Phys.* 105 (1996) 10189.
- [14] W.W. Harper, D.J. Clouthier, *J. Chem. Phys.* 106 (1997) 9461.
- [15] D.L. Michalopoulos, M.E. Geusic, P.R.R. Langridge-Smith, R.E. Smalley, *J. Chem. Phys.* 80 (1984) 3556.
- [16] S. Gerstenkorn, P. Luc, Atlas du Spectre D'Absorption de la Molecule d'Iode (Editions du CNRS, Paris, 1978); S. Gerstenkorn, P. Luc, *Rev. Phys. Appl.* 14 (1979) 791.
- [17] H. Knoeckel, E. Tiemann, Program IodineSpec5, <<http://www.iqo.uni-hannover.de>>.
- [18] PGOPHER, a Program for Simulating Rotational Structure, C. M. Western, University of Bristol, <<http://pgopher.chm.bris.ac.uk>>.
- [19] PGOPHER, A Program for Simulating Rotational, Vibrational and Electronic Spectra, C. M. Western, *J. Quant. Spectrosc. Radiat. Transf.* 186 (2016) 221–242.
- [20] S.G. He, D.J. Clouthier, *Comput. Phys. Commun.* 178 (2008) 676.
- [21] P.P. Power, *Chem. Rev.* 99 (1999) 3463.
- [22] W.W. Harper, K.W. Waddell, D.J. Clouthier, *J. Chem. Phys.* 107 (1997) 8829.
- [23] S. Bailleux, M. Bogey, J. Breidung, H. Burger, R. Fajgar, Y. Liu, J. Pola, M. Senzlober, W. Thiel, *Angew. Chem. Int. Ed. Engl.* 35 (1996) 2513.
- [24] S. Bailleux, M. Bogey, J. Demaison, H. Burger, M. Senzlober, J. Breidung, W. Thiel, R. Fajgar, J. Pola, *J. Chem. Phys.* 106 (1997) 10016.
- [25] T.J. Butenhoff, E.A. Rohlfing, *J. Chem. Phys.* 95 (1991) 3939.
- [26] R. Stegmann, G. Frenking, *J. Comput. Chem.* 17 (1996) 781.
- [27] C. Léonard, private communication.
- [28] Unfortunately, this constant was inadvertently left out of Table 5 of ref. 10.